Electric Field Waveforms of Very Close Negative Cloud-to-Ground Flashes

Shamsul Ammar Shamsul Baharin and Mohd Riduan Ahmad*

Atmospheric and Lightning Research Laboratory, Broadband and Networking Research Group (BBNET), Centre for Telecommunication and Research Innovation (CeTRI), Fakulti Kejuruteraan Elektronik dan Kejuruteraan Komputer (FKEKK), Universiti Teknikal Malaysia Melaka (UTeM), 76100 Durian Tunggal, Melaka, Malaysia

**Email: riduan@utem.edu.my*

Article Information

Received:
18 October 2020

Received in revised form:
20 November 2020

Accepted:
5 December 2020

Volume 2, Issue 2, December 2020
pp. 115 – 120

Abstract

Negative cloud-to-ground brings down negative charge from cloud to ground. In this paper, observations of the characteristics of fast and slow electric field within reversal distance (less than 7-8 km from lightning sensor) are reported. A total of four negative cloud to ground flashes detected very close to our measurement site in Universiti Teknikal Malaysia Melaka on 12th November 2019 were selected for analysis. The captured waveforms are compared with the location data provided by Tenaga Nasional Berhad Research (TNBR) for validation purposes. It can be observed that electric field changes of stepped leader and return stroke are always positive whether beyond or within reversal distance. Meanwhile, for cloud activities, the electric field change is always negative within reversal distance.

Keywords: *cloud to ground flash; electric field; lightning*

I. Introduction

LIGHTNING flash can be divided into two main types which are cloud flash (intra-cloud or IC is subtype of cloud flash) and cloud-to-ground (CG) flash. The type of lightning flash also depends on the type of cloud. In Malay Peninsula, cumulonimbus is the most common type of cloud. Negative cloud-to-ground (-CG) flash brings down negative charge from the cloud to the ground and started with initial breakdown (IB) inside the cloud followed by stepped leader discharges and lastly neutralization process from downward leader with upward leader through attachment process that causes immediate current surge known as return stroke (RS). The first study to observe ground-based measurements of electric fields of thunderclouds was reported in [1-4] where they found that lightning discharges near the sensors causes negative electric field changes compared to far lightning flash with positive field changes. Besides, they also suggested that thunderclouds typically have negative charge below positive charge which is a configuration of positive dipole charge structure of cloud. Therefore, we are motivated to observe the same pattern of electric field change of very close tropical lightning flashes.

II. Reversal Distance

The ideal charge structure for cumulonimbus cloud is three vertically stacked point charges where positive at the top, negative at the middle and additional pocket positive at the bottom located above a conducting ground (earth's surface) as illustrated in Fig. 1. From Fig. 1, Q is the quantity of electric charge in Coulomb (C) while H is the height of the charge region approximately from the ground.

The electric field intensity E can be found by replacing the conducting ground with three image charges. Based on Figure 2, the total electric field is sum of six vectors which are three from actual charges and three from their images by using principle of superposition and can be explained in Equation 1. From Fig. 2, H is height of the charge region to the ground, R is distance while α is the azimuth angle [5].

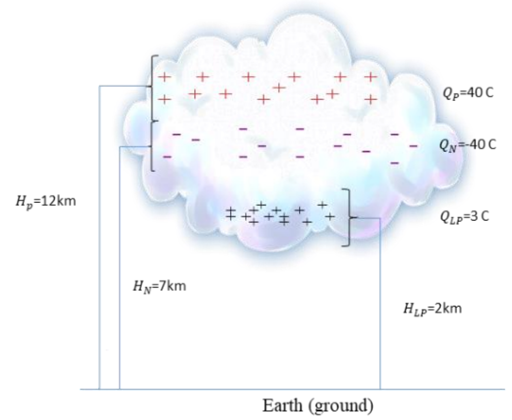

Figure 1:.Charge structure of a cumulonimbus cloud

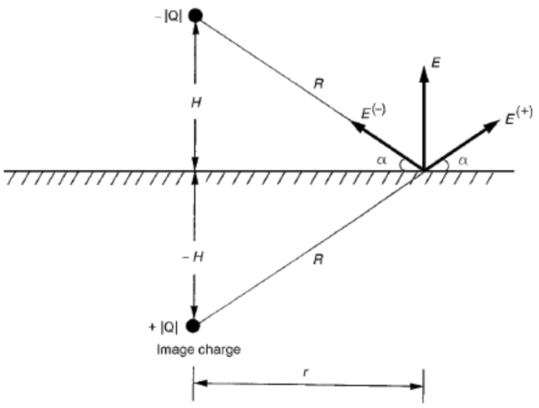

Figure 2. The method of image to find the total electric field

$$|E^{(-)}| = |E^{(+)}| = \frac{|Q|}{4\pi\varepsilon_0 (H^2 + r^2)} \quad (1)$$

The total normal field magnitude doubled either from the actual charge or its image due to the condition of the surface of ground is perfect conductor where the components of electric field tangential to the ground plane cancelling each other.

$$|E| = 2|E^{(-)}| \sin(\alpha) = \frac{|Q| H}{2\pi\varepsilon_0 (H^2+r^2)^{\frac{3}{2}}} \quad (2)$$

From Equation 2, it can be simplified as H and r ($|Q|$=constant) as follows:

$$|E| = k\frac{\sin\alpha}{R^2} \quad (3)$$

where k=$|Q|/(2\pi\varepsilon_0)$ and $R^2=H^2+r^2$.

As the value of E depends on r, if r equals to 0, the electric field dominated by the lower charge. When r increases to a certain distance, the contribution from the upper charge becomes dominant, and the total electric field (the sum of the contributions from the two charges) changes its polarity and the distance defined as reversal distance. For the case of two vertically stacked charges of equal magnitude but opposite polarity the reversal distance, D_0, is given by:

$$D_0 = [(H_p H_N)^{\frac{2}{3}} + \left(H_p^{\frac{2}{3}} + H_N^{\frac{2}{3}}\right)]^{1/2} \quad (4)$$

Figure 3 shows the electric field at ground due to the vertical tripole charge distributions of cloud. Based on Fig. 1, the main negative and main positive charges were set at 40 C with 7 and 12 km above ground, respectively. Meanwhile, the pocket positive is 2 km above ground with magnitude of 3 C. The total electric field exhibits polarity reversals dependent on the distance. Fig. 3 also shows the contributions to the total electric field from each of the three charges [5].

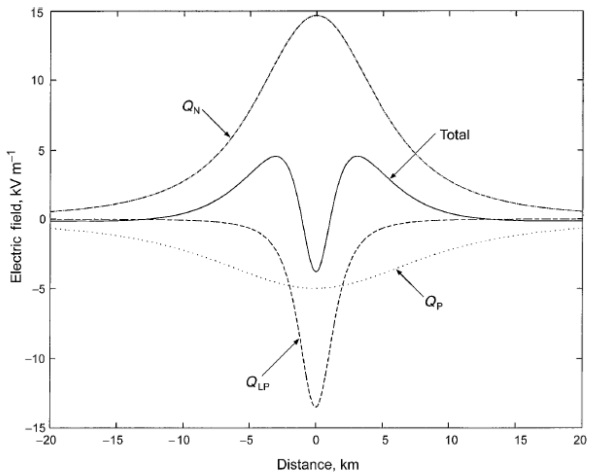

Figure 3. The electric field at ground based on tripole charge distribution cloud [5]

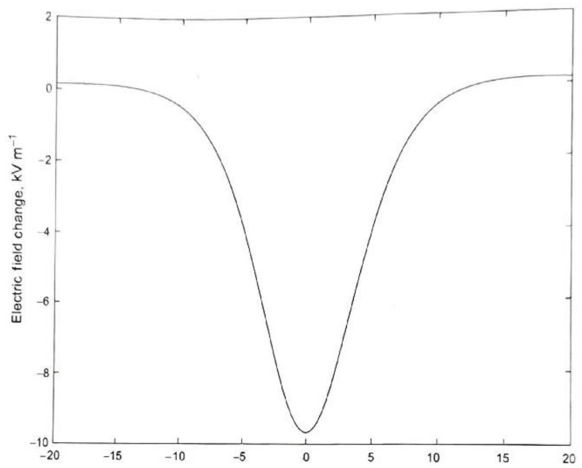

Figure 4. Electric field change at close distance is negative, but far distances it is positive ([10])

III. Materials and Methods

The measurement campaign was conducted during rainy season in November 2019. Four close -CG lightning flashes were chosen on 12th November 2019. Lightning signal that beamed on the sensors are in analog form. Thus, PicoScope 5000 series is used as digitizer to convert the analog signal into digital signal. The waveforms could be monitored remotely using the computer. Analysis was also done from the computer as it was more convenient by using PicoScope 6 software. The waveform was sampled with sampling rate of 125 Mega Samples/second. The visual diagram of the measurement set up is as shown in Fig. 5. Two buffer circuits were deployed with capacitive parallel plate antennas [6-8]. Fast-field (FF) buffer circuit operating frequency is between several Hertz up to 3 Mz with decay time constant 13 ms while Slow-field (SF) buffer circuit operated between a few Hertz to 1 kHz with decay time constant 1s. Circuit diagram of the FF buffer circuit is displayed in Fig. 2. The difference between FF and SF buffer circuit is the value of C1, 15 pF and 0.1 µs, respectively for FF and SF buffer circuits. The list of components to construct the buffer circuits is shown in Table 1. The type of lightning flashes measured were determined by using FF record.

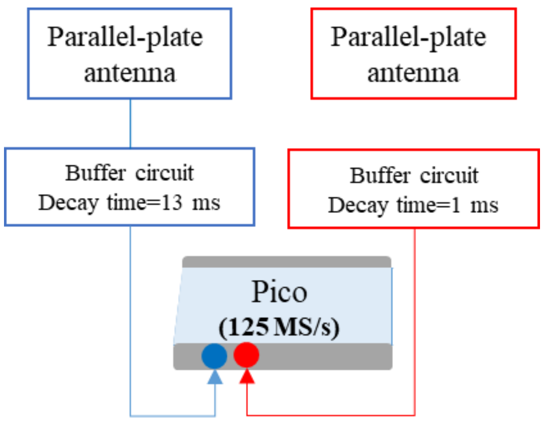

Figure 5. Visual diagram of the measurement setup

Table 1: List of components

Fast & Slow Field	
Component	Unit
100 MΩ resistor	2
100 Ω resistor	4
50 Ω resistor	4
IC OPA 633 KP	2
Capacitor 15 pF	1
Capacitor 0.1 µF	4
Capacitor 10 nF	1

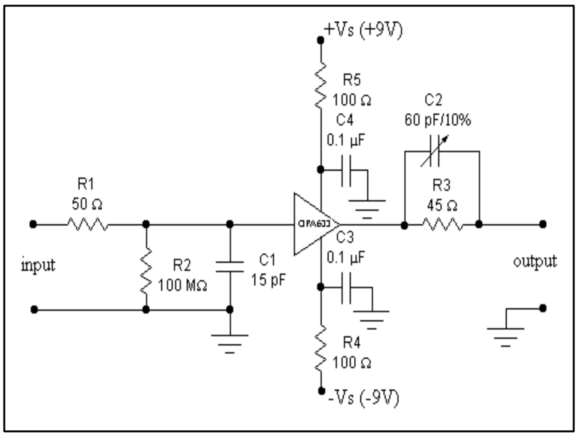

Figure 6. Circuit diagram of FF buffer circuit [9]

The antenna used to measure the electric field from lightning flashes is circular parallel plate antenna. The size of the antenna is calculated using Equation 5, where the antenna radius r_A=0.25m. The antenna is capable to capture radiation, static and induction component from lightning flashes by using fast and slow electric field system deployed during the measurement campaign. Capacitance value of the antenna is calculated using Equation 6, where ε_o is the permittivity of the space (8.8542×10^{-12}), A is area of the plates that obtain from Equation 5 and *d* is the gap between the plates which is 0.05m. Besides, the impedance of the antenna from 1 kHz to 100 kHz is calculated by using Equation 7 where *f* is the frequency value and *C* is the capacitance value. The value and the response of the impedance can be referred in Table 2 and Fig. 7. Example of completed antenna is shown in Figure 8 (a) and (b).

$$A = \pi r_A^2 \quad (5)$$

$$C = \frac{(\varepsilon_o A)}{d} \quad (6)$$

$$Z_C = \frac{1}{2\pi f C} \quad (7)$$

Table 2: Value of impedance of circular parallel plate antenna

Frequency (kHz)	Impedance, Zc (Ω)
10	4577316.24
20	416119.66
30	217967.44
40	147655.36
50	111641.86
60	89751.30
70	75037.97
80	64469.24
90	56510.08
100	50300.18

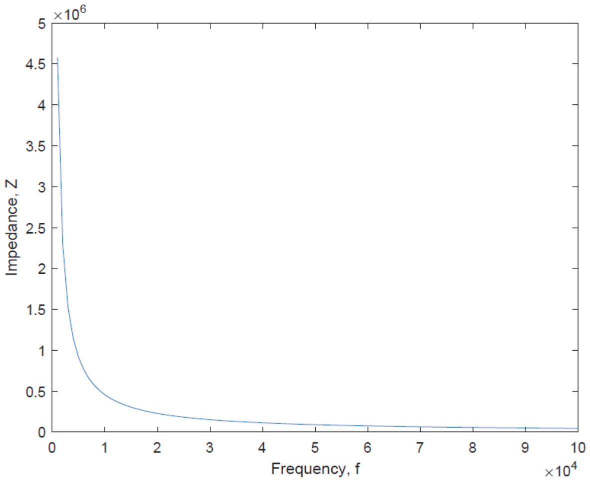

Figure 7 Impedance response of the antenna as a function of frequency

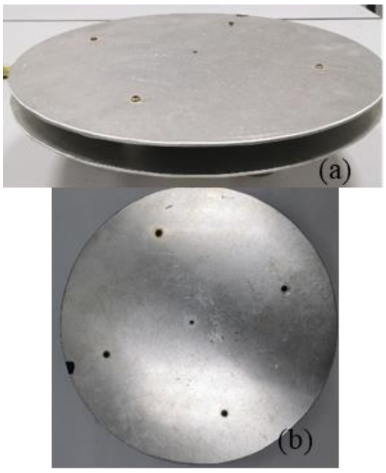

Figure 8. Circular parallel plate antenna (a): Side view with air gap (b): Top view

IV. Results and Discussions

A. Validation of Lightning Flash

A total of four -CG flashes within reversal distance (RD) during 12th November 2019 close to our lightning measurement system were chosen. The collected samples were validated by comparing with the data provided by Tenaga Nasional Berhad Research (TNBR) [10]. The locations of the first return stroke and distances from our sensors are presented in Fig. 9. The distances of the lightning strikes ranging between 1.936 and 4.196 km captured from 3:37:45 PM to 4:19:47 PM. The details for the -CG lightning flashes are presented in Table 3.

Table 3: Details of the -CG lightning flashes

Flash No.	Time (UTC+8)	Distance (km)
F1	15:37:45	2.152
F2	16:05:28	1.936
F3	16:07:15	3.137
F4	16:19:47	4.196

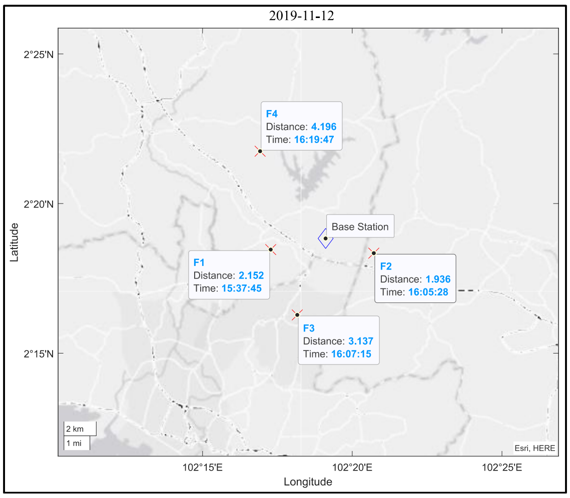

Figure 9. Locations of the first return strokes of CG lightning strikes to the location of our base station.

B. Observations of electric field change waveforms

The observations of the electric field waveforms for close -CG lightning flashes were done by analyzing the shape of the SF waveforms. Our measurement system consists of two sensors; FF (blue) and SF (red) as plotted in Fig. 11 to 14. The analysis was conducted by comparing our SF records with the shape of electric field changes as reported by [11]. For -CG, the polarity of return stroke (RS) is positive according to atmospheric sign convention. Stepped leader (SL) and RS processes will maintain the reversed polarity, but initial breakdown (IB) and cloud activities discharges will be negative polarity within RD as analytically discussed in [12].

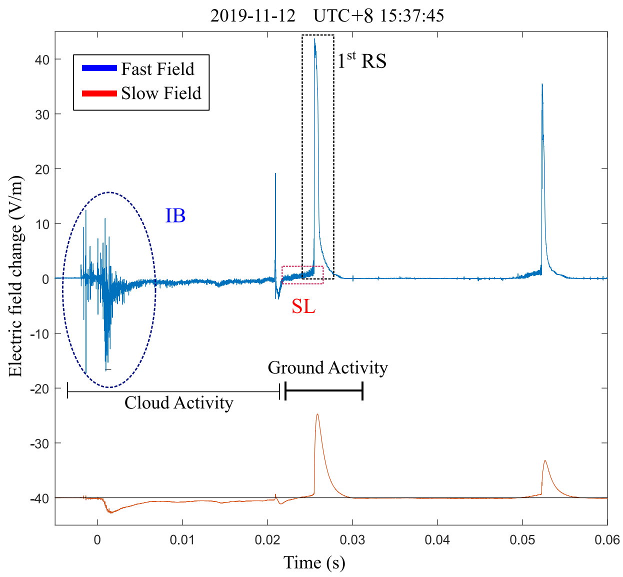

Figure 11. FF (blue) and SF (red) records for F1

The distance from our sensor to the location of RS strike for F1 is 2.152 km. From Figure 11, the zero line is denoted as horizontal line (black) from SF records. The electric field changes of initial breakdown (IB) process propagated near to the sensors within RD but, getting farther from the sensors (still within RD) during cloud activities until SL and RS discharge process took place. Notice that IB and cloud activities for SF records of -CG lightning flash is always negative but, the SL and RS are always positive.

Next, the SL and RS for F2 strikes 1.936 km from our sensors. From Fig. 12, the electric field change of IB is within RD. This is because the SF record always negative while positive during SL and RS. The propagation of electric change of IB and cloud flash is away from the sensors but still within RD. However, the electric change of leaders become closer to our sensors before the SL and RS occurred.

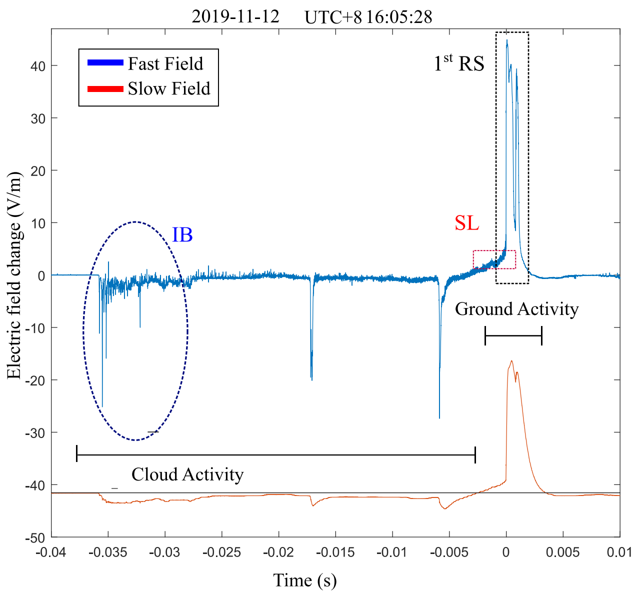

Figure 12. FF (blue) and SF (red) records for F2

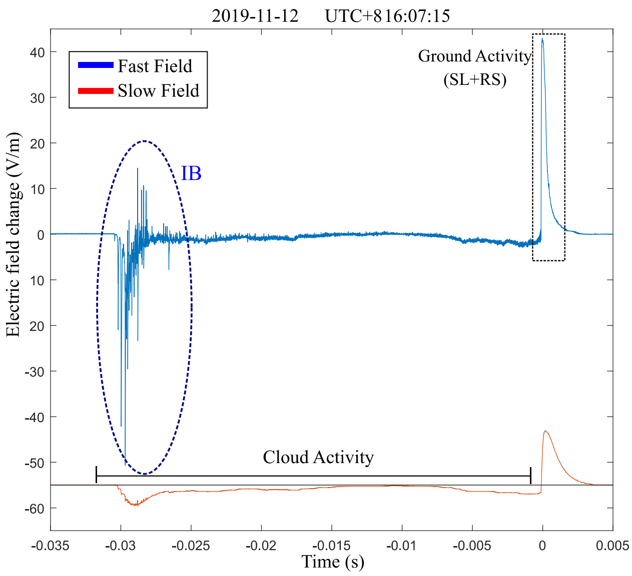

Figure 13. FF (blue) and SF (red) records for F3

Meanwhile, the distance of SL and RS that strikes the ground is 3.137 km away from our sensors for F3. It can be observed from Fig. 13 that during IB, the electric field change propagated closer to our sensors but becoming farther during cloud flash. However, electric field change during leader moving closer again to the sensors just before the SL and RS occurred.

Lastly, the SL and RS for F4 strikes the farthest from our sensors which is 4.196 km but still within RD. However, the electric field change during IB and cloud flashes occurred beyond RD as the electric change value is positive as shown in Fig. 14. The leaders gradually propagate passed the RD boarder around 7 to 8 km and strike 4.196 km from our sensor. This shows that cloud activities before SL and RS which is a part of -CG flash can occur beyond RD but propagate to strike within the RD.

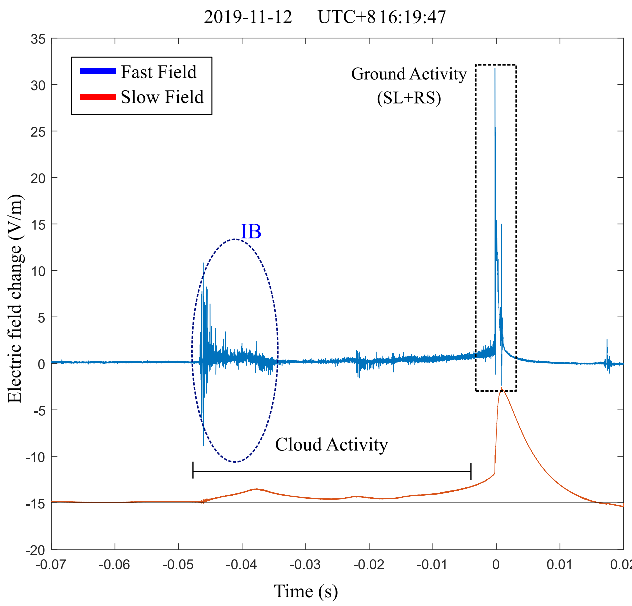

Figure 14. FF (blue) and SF (red) records for F4

V. Conclusions

In conclusion, this observation proved that electric field change within RD always negative and opposite if beyond RD. Meanwhile, the value for SL and RS always reversed the polarity of charges that propagating from the cloud to the ground (according to atmospheric sign convention). For future improvement, high frequency sensors could be installed to investigate the correlation between the characteristics of high frequency associated with the lightning flash within RD.

APPENDIX

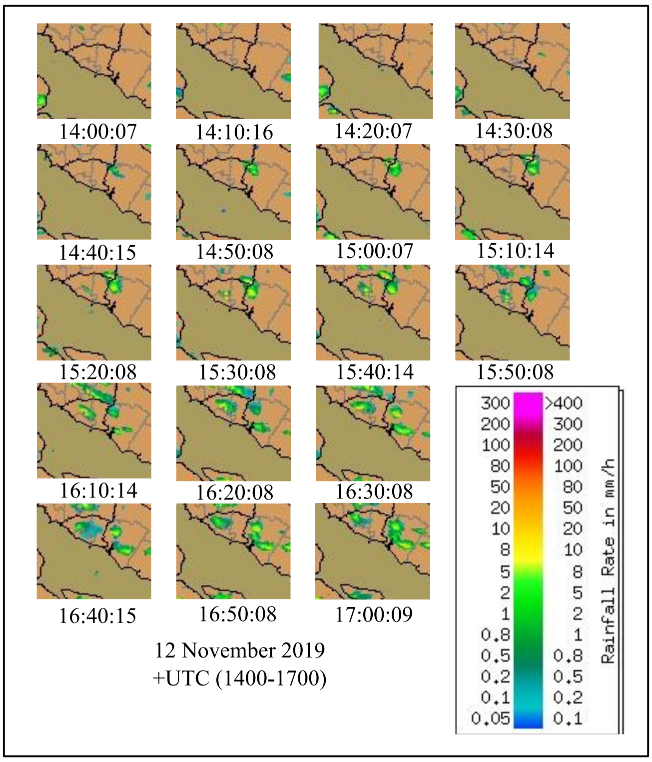

CAPPI radar format at 2 km altitude for Malay Peninsular focusing on area surrounding Melaka state and Malacca Strait for 3 hours Malaysia time UTC+8 on 12th November 2019. Adapted from official website of MMD. (This result shows the intensity of thundercloud when lightning happened, and it shows the movements of cloud for a period of 3 hours).

ACKNOWLEDGMENT

The authors would like to acknowledge the support provided by Centre for Telecommunication Research and Innovation (CeTRI), Fakulti Kejuruteraan Elektronik dan Kejuruteraan Komputer (FKEKK), Universiti Teknikal Malaysia Melaka (UTeM) and Ministry of Education Malaysia. This project is funded by Collaborative Research Grant (CRG) (PJP/2019/FKEKK-CETRI/CRG-S01707) and International Grant (ANTARABANGSA-UNSRI/2019/FKEKK-CETRI/A00022).

REFERENCES

[1] C.T.R. Wilson, "On some determinations of the sign and magnitude electric field discharges in lightning flashes", *Proceedings of the Royal Society of London. Series A, Containing Papers of a Mathematical and Physical Character*, vol. 92, no. 644, pp. 555-574, 1916.

[2] C.T.R. Wilson, "Investigations on lightning discharges and on the electric field", *Philosophical Transactions of the Royal Society of London. Series A, Containing Papers of a Mathematical or Physical Character*, vol. 221, no. 582-593, pp.73-115, 1921.

[3] C.T.R. Wilson, "Some thundercloud problems", *Journal of the Franklin Institute*, vol. 8, no. 1, pp.1-12, 1929.

[4] C.T.R. Wilson, (1956). "A theory of thundercloud electricity", *Proceedings of the Royal Society of London. Series A. Mathematical and Physical Sciences*, vol. 236, no. 1206, pp. 297-317, 1956.

[5] V.A. Rakov and M.A. Uman, Lightning: physics and effects, UK:Cambridge university press, 2003.

[6] M.H.M. Sabri, M.R. Ahmad, M.R.M. Esa, D. Periannan, B.Y. Seah, S. A. Mohammad, Z. Abdul-Malek, G. Lu, H. Zhang, N. Yusop, and V. Cooray, "Environmental analysis of quasi-static electric field changes of tropical lightning flashes", *Ekoloji*, vol. 28, no. 107, pp.373-378, 2019.

[7] M.R. Ahmad, M.R.M. Esa, V. Cooray, Z.A. Baharudin, P. Hettiarachchi, "Latitude dependence of narrow bipolar pulse emissions", *Journal of Atmospheric and Solar-Terrestrial Physics*, vol. 128, pp 40–45, 2015.

[8] B.Y. Seah, M.R. Ahmad, N.A. Shairi, D. Periannan, M.H.M. Sabri, M.Z.A.A. Aziz, M.M. Ismail, M.R.M. Esa, S. A. Mohammad, Z. Abdul-Malek, and N. Yusop, "The Performance Evaluation of Capacitive Antenna with Various Structures and Permittivity Values" in *International Conference on Electrical Engineering and Computer Science (ICECOS)*, Bangka, pp. 457-460, 2018.

[9] D.U.J. Sonnadara, C.M. Edirisinghe and I.M.K. Fernando, "Construction of a high-speed buffer amplifier to measure lightning generated vertical electric fields", in *Proceedings of the Technical Sessions*, Sri Lanka, 2019.

[10] M.H.M. Sabri, M.R. Ahmad, M.R.M. Esa, D. Periannan, G. Lu, H. Zhang, V. Cooray, E. Williams, M.Z.A.A. Aziz, Z. Abdul-Malek, and A.A. Alkahtani, "Initial electric field changes of lightning flashes in tropical thunderstorms and their relationship to the lightning initiation mechanism", *Atmospheric research*, vol. 226, pp.138-151, 2019.

[11] V.A. Rakov, and M.A. Uman, "Electrical structure of lightning-producing clouds", *Lightning: Physics and Effects*, pp. 687, 2004.

[12] Marshall, T., Stolzenburg, M., Karunarathna, N. and Karunarathne, S., "Electromagnetic activity before initial breakdown pulses of lightning", *Journal of Geophysical Research: Atmospheres*, vol. 119, no. 22, pp. 12-558, 2014.